Design of Circular Polarization Array Antenna Based on Uniform Rotating Feed Network

Qijia Zhou[1], Lulu Bei[1(✉)], Lei Chen[1], and Kai Huang[2]

[1] School of Information and Electrical Engineering, Xuzhou Institute of Technology, Xuzhou, China
[2] JiangSu XCMG Information Technology Co., Ltd., Xuzhou 221008, China

Abstract. In order to improve the quality of the receiving and transmitting signals in the underground wireless communication system, the circular polarization antenna located at the front of the communication system is studied. A 16 array circularized reading and writing antenna with a center frequency of 2.4 GHz is proposed for the formation of a center-shaped square-shaped circular-polarized patch radiation structure based on two-stage rotation. The structural composition and working principle of the microband antenna are introduced, and the function differential theory is applied to the feed antenna network. Finally, the simulation and experiments proved that the antenna has the advantage of having a high front-to-back ratio, and improved the performance of the antenna.

Keywords: Communication systems · Circular polarization · Microband antennas · Feed networks

1 Introduction

The circularly polarized microstrip antenna is thin in profile, small in volume, light in weight, conformable and easy to integrate. It is widely used in mobile communication, satellite communication, radar, WLAN, RFID and other communication occasions [1–6]. In coal mine wireless communication, it is necessary for the antenna to have good penetration and anti-multipath ability to coal dust and water mist. The circularly polarized antenna has two orthogonal fields, horizontal and vertical. The circularly polarized antenna has better penetrability than the linearly polarized antenna in coal seam water mist under the same power [7–12]. Circular polarization can be divided into left-handed polarization and right-handed polarization. The antenna can only receive signals in the same polarization direction. In the process of underground transmission, the signal is easy to be reflected by obstacles, changes the polarization direction, and is not received by the original polarization direction antenna. In the underground environment of coal mine, it can be used as an effective means of anti-multipath [13–17]. To sum up, the design of microstrip circularly polarized antenna with small size, easy integration, wide frequency band and high performance is the research direction of coal mine underground wireless communication [18–25].

H. Song and D. Jiang (Eds.): SIMUtools 2020, LNICST 370, pp. 363–370, 2021.
https://doi.org/10.1007/978-3-030-72795-6_30

In order to improve the quality of receiving and transmitting signals of underground wireless communication system, the circular polarization antenna at the front end of the communication system is studied. A 16-array circular polarization reading and writing antenna with a central frequency of 2.4 GHz is proposed based on the two-stage rotation of the corner cut square circular polarization patch radiation structure [26–30]. The power divider theory is applied to the antenna feed network to improve the performance of the antenna. In this paper, the design method of circularly polarized antenna is proposed, and its simulation and test are carried out [31–35].

2 Structure of Array Circular Polarization Antenna

The circularly polarized array antenna designed in this paper is shown in Fig. 1. It can be seen that the antenna is composed of two-stage rotary feed network inside and between subarrays and 16 square tangent circularly polarized radiation patches. The RF signal is fed into the energy signal through the central feeding point, and then fed through the internal one quarter T-type network. The signal is divided into four channels with the same amplitude and the phase lag of 90° in turn. Then each signal is fed into four tangent circular polarized radiation patches through a four-part T- type feed network. It can be seen that the antenna consists of an internal T-type feed network and four external T-type feed networks to form the whole two-stage rotating feed network, and then 16 channels of signals are fed into 16 square tangent circular polarized radiation patches [36–39].

The array antenna is designed with microwave sheet F4B, the thickness of the media substrate is H_0s $= 1.5$ mm. The dielectric constant is $\varepsilon_r = 2.65$, and the media loss angle tangent value is 0.001. The array unit uses a cut-angle square patch for circular polarization radiation, with the right-angle driven by the cut triangle being $T_0 = 2.9$ mm, and the patch cell edge length being $W_0 = 36$ mm. Inside the subarray, the distance between the cell patch is $D_1 = 48$ mm, between the two subarrays, the distance between the adjacent cell patch is $D_1 = 48$ mm, and the edge length of the entire array antenna is $K_0 = 340$ mm.

3 Antenna Production and Experiments

Model and optimize the designed circularly polarized microband antenna based on the T-junction 16 array using hf-frequency electromagnetic simulation software HFSS, and then use a printed circuit board to make the physical image of the antenna as shown in Fig. 2.

The echo loss and far-field radiation performance of the antenna were tested using Agilent's vector network analyzers E8363B and SATIMO's darkroom test system SG24, respectively, with results shown in Fig. 3, 4 and 5. Figure 3 is the echo loss of the antenna, Fig. 4 is the radiation gain in the positive direction of the antenna z axis, and Fig. 5 is the axis ratio of the antenna z axis in the positive direction.

As shown in Fig. 3, the simulation frequency range of antenna return loss greater than 10 dB is 2.41–2.53 GHz, and the relative bandwidth is 4.9%; the corresponding test frequency range is 2.35–2.55 GHz, and the relative bandwidth is 8.2%. In terms of return loss, the test result is slightly better than the simulation result. It can be seen

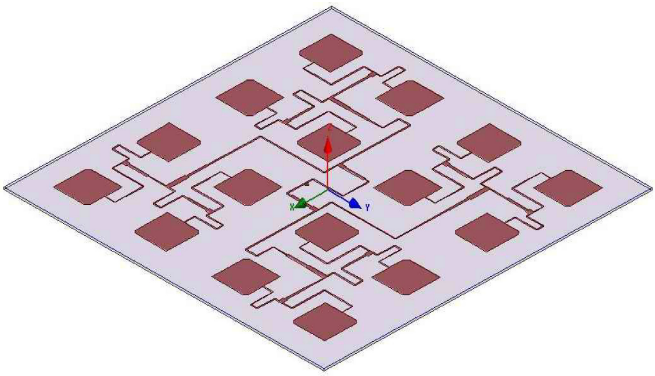

(a) Antenna 3D structural diagram

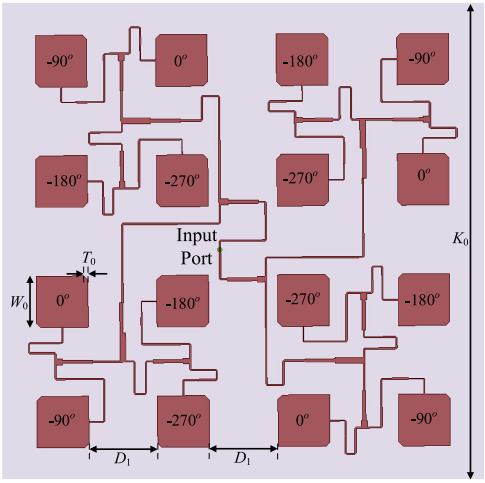

(b) Antenna Top View

Fig. 1. Antenna structure

from Fig. 4 that the simulated peak gain of the antenna is 18.75 dBi, the corresponding frequency point is 2.465 GHz, the tested peak gain is 17.60 dBi, and the corresponding frequency point is 2.472 GHz. In the frequency band 2.35–2.55 GHz, the simulated and tested gains are greater than 9.5 dbi. It can be seen from Fig. 5 that the simulation-3 dB axial ratio frequency range of the antenna is 2.42–2.51 GHz, with a relative bandwidth of 3.7%; the corresponding test working frequency range is 2.412–2.516 MHz, with a relative bandwidth of 4.2%; the above simulation and test results are basically consistent. The antenna is simulated and tested at 2.45 GHz, and the radiation patterns of XOZ and YOZ are obtained, as shown in Fig. 6. The test results show that in the XOZ plane and YOZ plane, the half power beam of the antenna is the same, both are 18° (−10°–8°). It can be seen that the simulation and test results of the antenna are very similar.

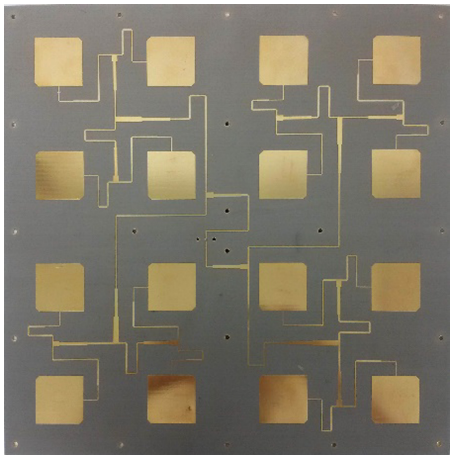

Fig. 2. Fabricated antenna structure

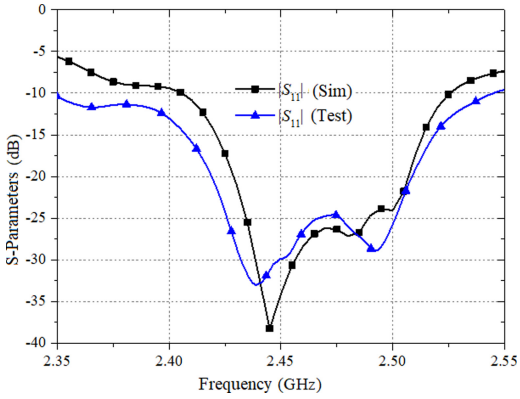

Fig. 3. Simulated and measured return loss

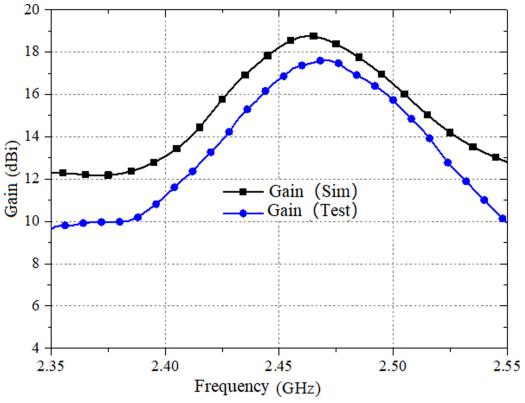

Fig. 4. Simulated and measured antenna gain

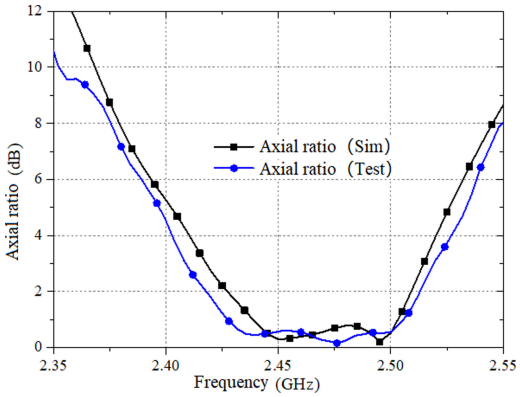

Fig. 5. Simulated and measured axial ratio

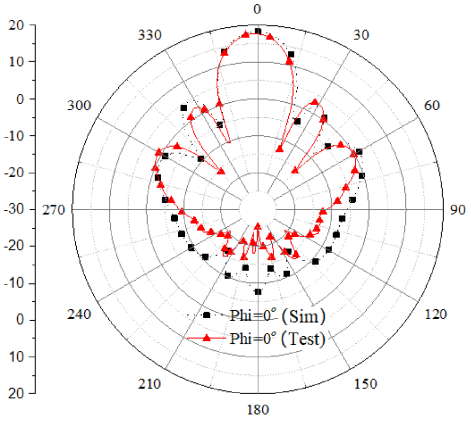

(a) Radiation pattern of XOZ plane at 2.45GHz

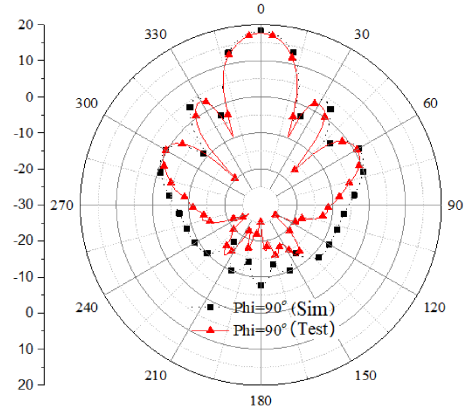

(b) Radiation pattern of YOZ plane at 2.45GHz

Fig. 6. Simulated and measured results of radiation pattern

4 Conclusion

In summary, the array antenna is mainly based on two-stage rotating symmetrical structure, square angled circular polarization patch, low-cost low-loss sheet to achieve high-performance RFID reading and writing array antenna. Taking into account the complexity and performance of the design, the feed network adopts the T-type Power Divider, phase shifter and impedance matcher cascade to realize the antenna structure of the feed network and the radiation patch co-face, which not only improves the front-to-front ratio, but also helps to reduce the complexity of antenna design and processing and assembly time and cost. The test results show that the echo loss of the antenna is better than 24.5 dB, the axis ratio is better than 0.5 dB, the peak gain is 17.8 dB, and the front and rear ratio is 30 dB. Ideal for the coal mine underground narrow environment RFID long-distance reading and writing applications, has a good application prospects and economic benefits.

Funding. This work was supported in part by Xu Zhou Science and Technology Plan Project (Grant No. KC19003), Science and technology project of Jiangsu Provincial Department of housing and construction (Grant No. 2018ZD265) and Major projects of natural science research in Colleges and universities of Jiangsu Province (Grant No. 19KJA470002).

References

1. Dehnavi, M.S., Razavi, S.M.J., Armaki, S.H.M.: Improvement of the gain and the axial ratio of a circular polarization microstrip antenna by using a metamaterial superstrate. Microw. Opt. Technol. Lett. **61**(8), 2261–3226 (2019)
2. Dai, H., Wang, X., Xie, H., Xiao, S., Luo, J.: Spatial polarization characteristics of aperture antenna. In: Spatial Polarization Characteristics of Radar Antenna, pp. 57–131. Springer, Singapore (2019). https://doi.org/10.1007/978-981-10-8794-3_3
3. Wang, F., Jiang, D., Qi, S.: An adaptive routing algorithm for integrated information networks. China Commun. **7**(1), 196–207 (2019)
4. Huo, L., Jiang, D., Qi, S., et al.: An AI-based adaptive cognitive modeling and measurement method of network traffic for EIS. Mobile Networks and Applications (2019)
5. Huo, L., Jiang, D., Lv, Z., et al.: An intelligent optimization-based traffic information acquirement approach to software-defined networking. Comput. Intell. **36**, 1–21 (2019)
6. Das, A., Mandal, D., Kar, R.: An optimal far-field radiation pattern synthesis of time-modulated linear and concentric circular antenna array. Int. J. Numer. Model. Electron. Netw. Devices Fields **32**(3), e2658 (2019)
7. Yassini, A.E., Aguni, L., Ibnyaich, S., et al.: Design of circular patch antenna with a high gain by using a novel artificial planar dual-layer metamaterial superstrate. Int. J. RF Microw. Comput. Aided Eng. **29**(7), e21939 (2019)
8. Debbarma, K., Bhattacharjee, R.: Matched feeds for offset reflector antenna using circular microstrip patch antenna. Int. J. RF Microw. Comput. Aided Eng. **29**(3), e21909 (2019)
9. Qi, S., Jiang, D., Huo, L.: A prediction approach to end-to-end traffic in space information networks. Mobile Networks and Applications (2019)
10. Jiang, D., Zhang, P., Lv, Z., et al.: Energy-efficient multi-constraint routing algorithm with load balancing for smart city applications. IEEE Internet Things J. **3**(6), 1437–1447 (2016)
11. Jiang, D., Li, W., Lv, H.: An energy-efficient cooperative multicast routing in multi-hop wireless networks for smart medical applications. Neurocomputing **220**(2017), 160–169 (2017)

12. Hatami, A., Naser-Moghadasi, M.: Split ring resonator metamaterial loads for compact Hepta band printed inverted F antenna with circular polarization. Microw. Opt. Technol. Lett. **60**(10), 2552–2559 (2018)
13. Bagheroghli, H., Zaker, R.: Double triangular monopole-like antenna with reconfigurable single/dual-wideband circular polarization. Int. J. RF Microw. Comput. Aided Eng. **28**(6), e21267 (2018)
14. Jiang, D., Huo, L., Lv, Z., Song, H., Qin, W.: A joint multi-criteria utility-based network selection approach for vehicle-to-infrastructure networking. IEEE Trans. Intell. Transp. Syst. **19**(10), 3305–3319 (2018)
15. Jiang, D., Huo, L., Li, Y.: Fine-granularity inference and estimations to network traffic for SDN. PLoS ONE **13**(5), 1–23 (2018)
16. Wang, Y., Jiang, D., Huo, L., Zhao, Y.: A new traffic prediction algorithm to software defined networking. Mobile Networks and Applications (2019)
17. Yuwono, R., Hidayatullah, B.R., Dahlan, E.A., et al.: Design of electromagnetic wave pollutant reducing device using rectenna and circular polarization microstrip antenna. Adv. Sci. Lett. **24**(1), 576–580 (2018)
18. Li, W., Leung, K.W., Yang, N.: Omnidirectional dielectric resonator antenna with a planar feed for circular polarization diversity design. IEEE Trans. Antennas Propag. **66**(3), 1189–1197 (2018)
19. Zhang, L., Gao, S., Luo, Q., et al.: Inverted-S antenna with wideband circular polarization and wide axial ratio beamwidth. IEEE Trans. Antennas Propag. **65**(4), 1740–1748 (2017)
20. Jiang, D., Wang, Y., Lv, Z., Wang, W., Wang, H.: An energy-efficient networking approach in cloud services for IIoT networks. IEEE J. Sel. Areas Commun. **38**(5), 928–941 (2020)
21. Jiang, D., Wang, W., Shi, L., Song, H.: A compressive sensing-based approach to end-to-end network traffic reconstruction. IEEE Trans. Netw. Sci. Eng. **7**(1), 507–519 (2020)
22. Jiang, D., Huo, L., Song, H.: Rethinking behaviors and activities of base stations in mobile cellular networks based on big data analysis. IEEE Trans. Netw. Sci. Eng. **7**(1), 80–90 (2020)
23. Shahid, H., Khan, M.T.A., Tayyab, U., et al.: RFID antenna design for circular polarization in UHF band. SPIE Defense + Security (2017)
24. Fukusako, T., Yamauchi, R.: Broadband waveguide antenna using L-shaped probe for wide-angle circular polarization radiation. IEICE Commun. Express **6**, 53–54 (2017)
25. Jiang, D., Wang, Y., Lv, Z., Qi, S., Singh, S.: Big data analysis based network behavior insight of cellular networks for industry 4.0 applications. IEEE Trans. Ind. Inform. **16**(2), 1310–1320 (2020)
26. Chen, L.N., Xie, H.H., Jiao, Y.C., Zhang, F.S.: A novel 4:1 unequal dual-frequency Wilkinson power divider. In: 2010 International Conference on Microwave and Millimeter Wave Technology (ICMMT), pp. 1290–1293. IEEE (2010)
27. Mohra, A., Alkanhal, M.: Dual band Wilkinson power dividers using T-sections. J. Microw. Optoelectron. Electromagn. Appl. **7**(2), 83–90 (2008)
28. Li, X., et al.: A novel design of dual-band unequal Wilkinson power divider. Prog. Electromagn. Res. C **12**, 93–100 (2010)
29. Wu, L., Yilmaz, H., Bitzer, T., et al.: A dual-frequency Wilkinson power divider: for a frequency and its first harmonic. IEEE Microw. Wirel. Compon. Lett. **15**(2), 107–109 (2005)
30. Sakagami, I., Wang, X., Takahashi, K., et al.: Generalized two-way two-section dual-band Wilkinson power divider with two absorption resistors and its miniaturization. IEEE Trans. Microw. Theory Tech. **59**(11), 2833–2847 (2011)
31. Ahn, H., Kim, B.: Toward integrated circuit size reduction. Microw. Mag. **9**(1), 65–75 (2008)
32. Monzon, C.: A small dual-frequency transformer in two sections. IEEE Trans. Microw. Theory Tech. **51**(4), 1157–1161 (2003)

33. Oraizi, H., Sharifi, A.R.: Optimum design of a wideband two-way Gysel power divider with source to load impedance matching. IEEE Trans. Microw. Theory Tech. **57**(9), 2238–2248 (2009)
34. Zysman, G., Johnson, A.K.: Coupled transmission line networks in an inhomogeneous dielectric medium. IEEE Trans. Microw. Theory Tech. **17**(10), 753–759 (1969)
35. Chongcheawchamnan, M., Patisang, S., Srisathit, S., et al.: Analysis and design of a three-section transmission-line transformer. IEEE Trans. Microw. Theory Tech. **53**(7), 2458–2462 (2005)
36. Huang, J.: A technique for an array to generate circular polarization with linearly polarized elements. IEEE Trans. Antennas Propag. **34**(9), 1113–1124 (1986)
37. Zhi, N.C., Xianming, Q., Hang, L.C.: A universal UHF RFID reader antenna. IEEE Trans. Microw. Theory Tech. **57**(5), 1275–1282 (2009)
38. Pan, Y., Zheng, L., Liu, H.J., et al.: Directly-fed single-layer wideband RFID reader antenna. Electron. Lett. **48**(11), 607–608 (2012)
39. Sim, C., Chi, C.: A slot loaded circularly polarized patch antenna for UHF RFID reader. IEEE Trans. Antennas Propag. **60**(10), 4516–4521 (2012)